

FIELD QUALITY OF QUADRUPOLE R&D MODELS FOR THE LHC IR*

N. Andreev, T. Arkan, P. Bauer, R. Bossert, J. Brandt, D. Chichili, J. DiMarco, S. Feher, J. Kerby, M. Lamm, P. Limon, F. Nobrega, I. Novitski, T. Ogitsu, D. Orris, J. Ozelis, T. Peterson, G. Sabbi, P. Schlabach, J. Strait, C. Sylvester, M. Tartaglia, J. Tompkins, S. Yadav, A. Zlobin, Fermilab, IL
S. Caspi, R. Scanlan, Lawrence Berkeley National Laboratory, Berkeley, CA

Abstract

Superconducting quadrupole magnets operating in superfluid helium at 1.9 K, with 70 mm bore and nominal field gradient of 205 T/m at collision optics, are being developed by the US LHC Accelerator Project for the Interaction Regions of the Large Hadron Collider (LHC). A magnet model program to validate and optimize the design is underway. This paper reports results of field quality measurements of four model magnets.

1 INTRODUCTION

In order to achieve a luminosity of $10^{34} \text{ cm}^{-2}\text{s}^{-1}$ at the LHC, special quadrupole magnets are required for the final focusing triplets [1]. These magnets must provide a field gradient of 205 T/m over a 70 mm bore with sufficient cooling capacity to withstand the heavy heat load deposited by secondary particles from beam-beam collisions. At the same time, high field quality is required due to large and rapidly varying values of the β -function. A design based on two-layer coil geometry has been developed by a Fermilab-LBNL collaboration for inner triplet quadrupoles (MQXB). Five short models (HGQ01-HGQ05) have been fabricated. Four have been tested in superfluid helium at the Fermilab Vertical Magnet Test Facility. In this paper, field harmonics measured in the magnet straight section and in the end regions are presented and compared with calculations based on as-built magnet geometry and with preliminary field quality specifications.

2 MAGNET DESIGN

Figure 1 shows the magnet cross-section. The design is based on four two-layer coils connected in series, surrounded by collar and yoke laminations. No modifications to the design cross-section were made during the magnet model program, but different coil shimming schemes have been implemented in each model in order to obtain the desired coil modulus and prestress.

The end regions underwent several design changes during the model program. The five models built have a four-block end configuration. With respect to the design of HGQ01, the second-wound group of the outer coil was shifted by 2 cm in the positive z direction starting with

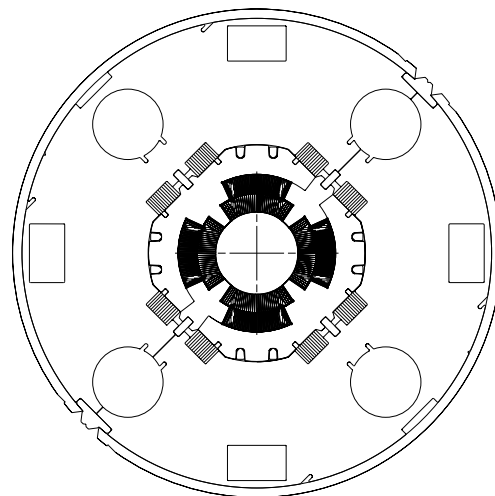


Figure 1: Magnet cross-section.

HGQ02 to reduce the peak field in the coil. A more compact design for the coil to coil joint in the lead end was introduced in HGQ03 and HGQ05. A new five-block configuration will be implemented in future models which will improve the mechanical stability of inner layer conductors during winding. The new design also reduces the peak field in the coil and significantly improves end field quality.

3 MEASUREMENT SYSTEM

Magnetic measurements presented in this paper were performed using a vertical drive, rotating coil system. Probes used have a main tangential winding for measurement of higher order harmonics as well as specific dipole and quadrupole windings for measurement of the lowest order components of the field. These windings also allow for bucking the large dipole and quadrupole components in the main coil signal. Most measurements presented in this paper were made with a coil of 40.6 mm nominal diameter and length 82 cm.

Coil winding voltages are read using HP3458 DVMs. An additional DVM is used to monitor magnet current. DVMs are triggered simultaneously by an angular encoder on the probe shaft, synchronizing measurements of field and current. Feed down of the quadrupole signal to the dipole is used to center the probe in the magnet.

* Work supported by the U.S. Department of Energy.

Table 1: Reference collision harmonics for MQXB

n	$\langle b_n \rangle$	$d(b_n)$	$\sigma(b_n)$	$\langle a_n \rangle$	$d(a_n)$	$\sigma(a_n)$
Straight section (magnetic length 4.76/5.56 m)						
3	.0	.3	.8	.0	.3	.8
4	.0	.2	.8	.0	.2	.8
5	.0	.2	.3	.0	.2	.3
6	.0	.6	.6	.0	.05	.1
7	.0	.05	.06	.0	.04	.06
8	.0	.03	.05	.0	.03	.04
9	.0	.02	.03	.0	.02	.02
10	.0	.02	.03	.0	.02	.03
Lead end (magnetic length 0.41 m)						
2	-	-	-	40.	-	-
6	2.	2.	.8	.0	.5	.2
10	-.2	.2	.1	.0	.1	.1
Return end (magnetic length 0.33 m)						
6	.0	1.2	1.	-	-	-
10	-.25	.25	.1	-	-	-

4 FIELD QUALITY ANALYSIS

In the straight section of the magnet, the field is represented in terms of harmonic coefficients defined by the power series expansion

$$B_y + iB_x = B_2 10^{-4} \sum_{n=1}^{\infty} (b_n + ia_n) \left(\frac{x + iy}{r_0} \right)^{n-1} \quad (1)$$

where B_x and B_y are the transverse field components, B_2 is the quadrupole field, b_n and a_n are the $2n$ -pole coefficients ($b_2=10^4$). The reference radius r_0 is 17 mm.

Table 1 shows the reference harmonics at collision for MQXB magnets (version 2.0). For each harmonic component, values of the mean, uncertainty in mean and standard deviation are listed. This table provides a common reference for the discussion of field quality issues from the viewpoint of magnet development, machine performance and IR systems layout. The goal of the R&D phase is to converge on a set of numbers satisfying these requirements that can be adopted as a field quality specification for magnet production. Preliminary results of beam tracking studies aimed at evaluating the impact of magnet field errors on LHC dynamic aperture indicate that the values listed in Table 1 are acceptable from the machine performance standpoint [2].

Due to the thick coil shims (up to 450 μm) needed to obtain the required pre-stress, allowed harmonics b_6 and b_{10} were large in HGQ01. Also, due to 80 μm differences in size between inner coils used in quadrant 1 and 3 and those used in quadrant 2 and 4 and the corresponding adjustments of shim thickness, non-zero systematic values appeared for harmonic components a_4 and a_8 . Since then, significant improvements have been made in the coil fabrication procedure. Adjustments have been made to curing cavity size, curing pressure, cable insulation scheme and bare cable size. The coil shim thickness was reduced by about a factor of 2 from each magnet to the next, and better

Table 2: Comparison of measured straight section harmonics (6 kA) with calculations based on as-built parameters.

n	HGQ01	HGQ02	HGQ03	HGQ05
b_6 , calc.	-4.24	-2.86	-1.39	-0.08
b_6 , meas.	-3.91	-1.54	-1.02	-0.30
b_{10} , calc.	-0.14	-0.09	-0.04	0.01
b_{10} , meas.	-0.10	-0.10	-0.04	0.01
a_4 , calc.	1.27	0.94	0.00	0.00
a_4 , meas.	2.00	0.53	0.32	0.19
a_8 , calc.	0.02	0.00	0.00	0.00
a_8 , meas.	0.02	0.02	0.03	0.00

uniformity in size and modulus from coil to coil has been achieved with field quality improving correspondingly as the conductor positions approach design values.

Table 2 shows a comparison between measured harmonics and calculations based on as-built parameters for the harmonic components b_6 , b_{10} , a_4 and a_8 . The measurements are made at a current of 6 kA where all non-geometric components (conductor magnetization, iron saturation, conductor displacement under Lorentz forces) are small. Calculations and measurements are generally in good agreement. A reduction of the errors of about one order of magnitude is observed from magnet HGQ01 to magnet HGQ05. In magnet HGQ05, all four harmonics are within the uncertainties specified by the reference table. Table 3 shows the measured straight section harmonics up to the 20-pole for all four models. In magnet HGQ05, all central harmonics are within one standard deviation of the random error specified in Table 1. From the values in Table 3, averages and standard deviations over the four models have been obtained for each component (Table 4). In the attempt to eliminate the effect of systematic errors due to coil shims, the values for b_6 , b_{10} , a_4 and a_8 in Table 4 have been obtained after taking the difference between measured values and those calculated based on as-built parameters (Table 2). All average values and standard deviations in

Table 3: Measured harmonics in straight section (6 kA).

n	HGQ01	HGQ02	HGQ03	HGQ05
b_3	0.36	-0.70	1.04	0.72
b_4	0.26	0.18	0.14	0.00
b_5	-0.29	0.09	-0.34	-0.04
b_6	-3.91	-1.54	-1.02	-0.30
b_7	-0.08	-0.01	-0.06	0.01
b_8	0.06	0.01	0.00	0.00
b_9	0.04	0.00	0.00	0.00
b_{10}	-0.10	-0.10	-0.04	0.01
a_3	0.27	0.55	-0.30	0.12
a_4	2.00	0.53	0.32	0.19
a_5	0.02	-0.17	0.26	0.05
a_6	-0.08	0.03	0.07	-0.03
a_7	-0.05	0.00	-0.03	0.01
a_8	0.02	0.02	0.03	0.00
a_9	0.01	-0.01	0.01	0.00
a_{10}	0.02	0.00	-0.01	0.00

Table 4: Average and standard deviation of harmonics

n	$\langle b_n \rangle$	$\sigma(b_n)$	$\langle a_n \rangle$	$\sigma(a_n)$
3	0.36	0.76	0.16	0.35
4	0.15	0.11	0.21	0.47
5	-0.15	0.20	0.04	0.18
6	0.46	0.63	0.00	0.07
7	-0.04	0.04	-0.02	0.03
8	0.02	0.03	0.01	0.02
9	0.01	0.02	0.00	0.01
10	0.01	0.02	0.00	0.01

Table 4 are within the limits specified in Table 1. Note the b_6 result is strongly influenced by the relatively large difference between calculation and measurements in a single magnet (HGQ02). Moreover, one can expect smaller variations in a magnet production series than those observed in the first few models of a new design.

Figure 2 shows the measured dodecapole in model HGQ05 along with calculations of geometric and dynamic effects. The magnet design provides good compensation of the saturation and Lorentz force effect, and the total change of the mean dodecapole between injection and operating current is very small. This is actually the case for all harmonics. In particular, the 6 kA measurements (Table 3) do not differ significantly from those taken at higher currents. A simulation of the conductor magnetization effect on the normal dodecapole agrees very well with HGQ05 measurements, assuming a systematic (geometric) shift of -0.3 units. The magnetization effect is similar for all magnets, as expected from the uniformity of conductor properties. One exception is a specific pattern which appeared in magnet HGQ02 and HGQ03 which show a larger effect on the first cycle after quench than during subsequent cycles.

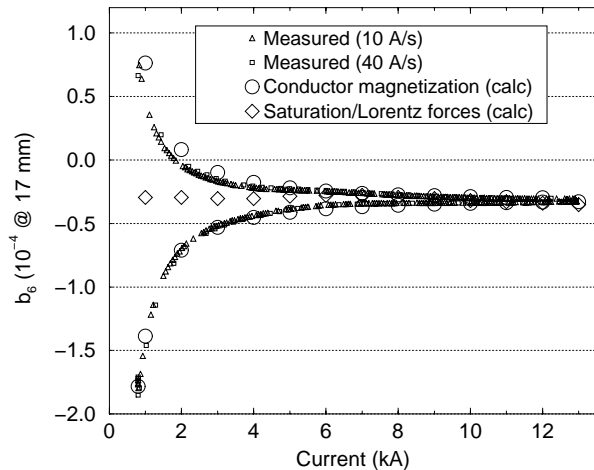


Figure 2: Normal dodecapole vs current (HGQ05).

The ramp-rate dependent distortions of the multipoles are weak (Figure 2), indicating a high average cross-contact resistance. Estimations of the cross-contact resistance based on AC-loss measurements of HGQ02 and HGQ03 yielded an average value of approximately $100 \mu\Omega$. No systematic ramp-rate dependent patterns on the multipoles

were observed. The lack of systematics in the ramp-rate effects indicates the large spread of the electrical cross-contact resistance typical of cables made of uncoated copper strands.

In the magnet end regions, additional terms (pseudo-multipoles) are required in the harmonic expansion for the local field. A simple expansion based on Equation 1 can however be applied to the total integral of the transverse field across the end region. The reference integration interval for harmonic coefficients in the magnet ends is defined to be $[-0.57, 0.25]$ m for the return end and $[1.31, 2.03]$ m for the lead end. This matches the length of the measurement probe. A comparison of measured and calculated harmonics in the magnet lead end is given in Table 5. Except for HGQ01, ¹ the end harmonics quoted in Table 5 are computed for the design geometry without considering the effect of coil shims, using program ROXIE [3]. For magnet HGQ02 and HGQ03, which used soft ULTEM end parts, thick mid-plane shims were applied to reach the desired pre-stress, resulting in a negative contribution to the dodecapole. In HGQ05, which uses G10 end parts, the thickness of the end shims was substantially reduced. This change in end shims, together with the reduction of the negative contribution from the straight section b_6 , contributes to the positive jump in the measured dodecapole of HGQ05 with respect to HGQ03. Although the present lead end b_6 is larger than specified in the table of reference harmonics, a reduction by about 30% of its systematic value is expected after implementation of the new 5-block end design.

Table 5: Calculated/measured harmonics in lead end.

n	HGQ01	HGQ02	HGQ03	HGQ05
b_6	3.1/2.9	5.5/4.2	5.4/3.8	5.4/8.0
b_{10}	-0.3/-0.3	-0.3/-0.2	-0.4/-0.4	-0.4/-0.2
a_6	0.5/0.1	0.4/0.2	-0.1/-0.3	-0.1/-0.6
a_{10}	-0.1/-0.1	0.0/0.0	0.0/0.0	0.0/0.0

5 CONCLUSIONS

Magnetic measurements of MQXB short models confirm design calculations for geometric harmonics, magnetization and Lorentz force effects. Refinements in magnet fabrication have significantly improved the field quality from each model to the next. Observed current-dependent effects are small. The systematic and random straight section harmonics are within specifications. The systematic normal dodecapole in the lead end is presently larger than the value listed in Table 1, but a significant improvement is expected after implementation of the new 5-block design.

6 REFERENCES

- [1] "LHC Conceptual Design", CERN AC/95-05 (LHC).
- [2] J. Wei, et al., this conference. N. Gelfand, this conference.
- [3] S. Russenschuck, Proc. ACES Symposium, Monterey, 1995.

¹A correction of -2 units was applied to the calculated b_6 integral for HGQ01 to include the contribution of mid-plane shims.